

# Dynamics of bright matter-wave solitons in a Bose–Einstein condensate with inhomogeneous scattering length

F Kh Abdullaev<sup>1,2</sup>, A Gammal<sup>3</sup> and Lauro Tomio<sup>2</sup>

<sup>1</sup> Physical-Technical Institute, Uzbek Academy of Sciences, 700084, Tashkent-84,

G Mavlyanov str, 2-b, Uzbekistan

<sup>2</sup> Instituto de Física Teórica, Universidade Estadual Paulista, Rua Pamplona, 145, 01405-900, São Paulo, Brazil

<sup>3</sup> Instituto de Física, Universidade de São Paulo, 05315-970 São Paulo, Brazil

Received 28 June 2003

Published 23 January 2004

Online at [stacks.iop.org/JPhysB/37/635](http://stacks.iop.org/JPhysB/37/635) (DOI: 10.1088/0953-4075/37/3/009)

## Abstract

We investigate dynamical effects of a bright soliton in Bose–Einstein condensed (BEC) systems with local and smooth space variations of the two-body atomic scattering length. It includes a discussion about the possible observation of a new type of standing nonlinear atomic matter wave in cigar-type traps. A rich dynamics is observed in the interaction between the soliton and an inhomogeneity. By considering an analytical time-dependent variational approach and also full numerical simulation of one-dimensional and three-dimensional Gross–Pitaevskii equations, we study processes such as trapping, reflection and transmission of the bright matter soliton due to the impurity. We also derive conditions for the collapse of the bright solitary wave, considering a quasi-one-dimensional BEC with attractive local inhomogeneity.

## 1. Introduction

Theoretical investigations of nonlinear collective excitations of matter waves actually became a very interesting and relevant subject with the experimental observations of Bose–Einstein condensation (BEC) in vapours of alkali-metal atoms [1]. One of the interesting forms of localized waves of atomic matter is the *solitons*—moving stationary nonlinear wavepackets. The solitons exist in quasi-1D geometry due to the balance between dispersion (a quantum pressure) and mean field nonlinearity in the Gross–Pitaevskii (GP) equation. As many properties of solitonic wavepackets are robust under perturbations, they can be relevant in atomic interferometry, atom lasers, etc [2]. Historically, *dark* solitons, objects with nontrivial topological properties, were first observed in BEC systems, where they can exist for repulsive two-atom interactions; i.e. for positive two-body scattering length  $a_s$ . They appear as *holes* in the background of the condensates [3].

The observation of solitons in BEC systems with negative two-body scattering length ( $a_s < 0$ ), the so-called *bright* solitons, is more complicated from the experimental point of view. The difficulty is related to the instability of condensates in two dimensions (2D) and three dimensions (3D), when the number of atoms  $N$  exceeds the critical limit  $N_c$ , which is typically a number of the order of 1500–6000 atoms for  $^7\text{Li}$ . This experimental limitation can be softened in the case of quasi-one-dimensional (1D) geometry, i.e. for a BEC in highly anisotropic cigar-type traps. We should observe that, for a true 1D system, one does not expect the collapse of the system with increasing number of atoms [4, 5]. However, it happens that a realistic 1D limit is not a true 1D system, with the density of particles still increasing due to the strong restoring forces in the perpendicular directions [6–8]. The validity of a true-1D picture in describing the dynamics of bright solitons is restricted to small values of the product between the number of particles and the scattering length [8]. Numerical applications to inhomogeneous BEC systems, in the 1D limit, have also been considered, recently, in [9].

Bright matter-wave solitons in a BEC with attractive interactions have been recently observed, as reported in [10, 11]. Theoretical models, explaining some aspects of observed phenomena, have been considered in [12, 13]. It should be noted that, in principle, the observation of bright matter-wave solitons is possible in a BEC with an optical lattice. The possibility of changing the sign of the effective dispersion in such lattices makes possible to generate bright solitons for repulsive condensates [14, 15]. Thus, it represents an interesting possibility of controlling the dynamics of bright matter-wave solitons. The control of dark solitons in a quasi-1D BEC with delta-function variation of a trap potential has been suggested in [9]. The interaction of bright solitons with local *linear* inhomogeneities has been investigated in the framework of nonlinear optics. An interesting effect of soliton reflection, in the NLS equation with linear attractive impurity, has been observed [16–18]. This effect was first observed for sine-Gordon kink scattered by the linear defect [19]. Recently, it has been suggested that the soliton parameters can be altered by changing the atomic scattering length through Feshbach resonance techniques. It was shown that this approach is effective for the compression of atomic solitons and nonlinear periodic waves [20–22].

For the control of the bright atomic soliton, we suggest using artificially induced inhomogeneities, by changing the *space* distribution of the atomic two-body scattering length. This variation can be achieved by using optical methods, as the optically induced Feshbach resonance suggested in [23]. According to the approach used in [23], the scattering length  $a_s$  can be varied by changing either the intensity or the detuning of a laser tuned near the photodissociation transition to a molecular state in the dimer. Another way of varying  $a_s$  is by an external magnetic field [24]. Mathematically, this leads to the appearance of a coordinate-dependent coefficient in the nonlinear term of the GP equation. Actually, our aim is to solve this problem for a condensate in a cigar-type trap using a full numerical solution of the GP formalism, obtained after a 1D reduction from the original 3D equation. To describe the dynamics of solitary atomic waves we use the time-dependent variational approach, which was successful in the description of BEC dynamics [7, 25]. In the last part of our work, the dynamics of the original 3D GP equation is also studied, considering a delta-like variation along the longitudinal direction, in order to verify the validity of the 1D reduction that was previously done. We consider both local and smooth space variation of the atomic scattering length. We should note that the GP equation with delta-like nonlinear inhomogeneity has a particular solution representing a *standing* nonlinear atomic matter wave. The soliton, trapped by the nonlinear impurity, evolves to this solution. We also estimate the values of the parameters for the observation of such a new type of nonlinear standing atomic matter wave.

The present work is organized as follows: in section 2, considering a reduction from 3D to 1D, we formulate the model for the quasi-1D BEC with nonlinear inhomogeneity and derive

the corresponding equations for the soliton parameters using the time-dependent variational approach. In section 3, we present the analysis of the fixed points, frequencies of oscillations for the width and centre of mass, considering inhomogeneities given by three models for the space variation of the scattering length: a Dirac-delta function (local impurity), a step function (transition between two media) and a smooth Gaussian function. In section 4, we consider the particular interesting case of nonlinear impurity mode. In the subsection 4.1, we include the numerical modelling of the system of ODE, with numerical simulations of the inhomogeneous GP equation. In the subsection 4.2, we present full 3D numerical dynamical results, which support the previous 1D results and show regions of parameters of inhomogeneity, when the condensate is stable. In section 5, we present our final remarks and conclusions.

## 2. Formulation of the model

The mean field equation for a Bose–Einstein-condensed system, trapped by a harmonic potential, is given by the following GP equation:

$$i\hbar \frac{\partial}{\partial t} \Psi(\vec{r}, t) = \left[ -\frac{\hbar^2}{2m} \nabla^2 + \frac{m}{2} (\omega_1^2 x_1^2 + \omega_2^2 x_2^2 + \omega_3^2 x_3^2) + \frac{4\pi\hbar^2 a_s}{m} |\Psi(\vec{r}, t)|^2 \right] \Psi(\vec{r}, t), \quad (1)$$

where  $a_s$  is the atomic scattering length,  $m$  is the mass of the atom and the wavefunction  $\Psi \equiv \Psi(\vec{r}, t)$  is normalized to the number of particles  $N$ . In the present work, we assume a cylindrical highly anisotropic trapped potential, such that  $\omega_{\perp} \equiv \omega_1 = \omega_2 \gg \omega_3$ . The scattering length is assumed having a space variation along the  $x_3$  axis given by  $a_s \equiv a_{s0} + \delta a_{s0} = a_{s0}[1 + \epsilon f(x_3/l_{\perp}, l_{\epsilon})]$ , where  $\epsilon$  is the effective strength of the impurity along the  $x_3$  axis,  $l_{\epsilon}$  is the inhomogeneity scale that will be defined by  $f$  and  $a_{s0}$  is the scattering length when  $\epsilon = 0$ . As  $\omega_{\perp} \gg \omega_3$ , one can approximate the field as [7]

$$\Psi(\vec{r}, t) = R(x_1, x_2)Z(x_3, t). \quad (2)$$

$R(x_1, x_2) \equiv R$  satisfies the 2D harmonic oscillator equation, that we assume is in the ground-state, normalized to 1:

$$\left[ -\frac{\hbar^2}{2m} \left( \frac{\partial^2}{\partial x_1^2} + \frac{\partial^2}{\partial x_2^2} \right) + \frac{m\omega_{\perp}^2}{2} (x_1^2 + x_2^2) \right] R = \hbar\omega_{\perp} R, \quad (3)$$

where

$$R = \frac{1}{\sqrt{\pi}l_{\perp}} \exp\left(-\frac{x_1^2 + x_2^2}{2l_{\perp}^2}\right), \quad \text{with } l_{\perp} \equiv \sqrt{\frac{\hbar}{m\omega_{\perp}}}. \quad (4)$$

Multiplying both sides of equation (1) by  $R$  and integrating over the transverse variables, using equations (2)–(4), we obtain

$$i\hbar \frac{\partial Z}{\partial t} = \left[ -\frac{\hbar^2}{2m} \frac{\partial^2}{\partial x_3^2} + \frac{m\omega_3^2 x_3^2}{2} + \hbar\omega_{\perp} + 2a_s \hbar\omega_{\perp} |Z|^2 \right] Z, \quad (5)$$

where  $Z \equiv Z(x_3, t)$  is normalized to the number of particles  $N$ . The condition of the validity of the quasi-1D approximation for BEC with attractive interaction is  $l_{\perp}/l_z \ll N|a_{s0}|/l_{\perp} \ll 1$ , where  $l_z = l_{\perp} \sqrt{\omega_{\perp}/\omega_3}$ .

Next, we redefine  $Z$  and the variables as

$$u(z, \tau) \equiv \sqrt{4|a_{s0}|} Z(x_3, t) e^{i\omega_{\perp} t}, \quad \tau \equiv \frac{\omega_{\perp} t}{2}, \quad z \equiv \frac{x_3}{l_{\perp}}, \quad \alpha \equiv \left( \frac{\omega_3}{\omega_{\perp}} \right)^2. \quad (6)$$

We redefine the function that will give us the space variation of the scattering length along the  $x_3$  axis as  $f(z)$ . Thus, after integrating in the transversal directions, and considering

the interesting case of attractive two-body scattering length ( $a_{s0} = -|a_{s0}|$ ), we obtain the following 1D NLSE:

$$i \frac{\partial u}{\partial \tau} = -\frac{\partial^2 u}{\partial z^2} + \alpha z^2 u - (1 + \epsilon f(z))|u|^2 u. \quad (7)$$

So,  $\epsilon > 0$  ( $\epsilon < 0$ ) refers to negative (positive) variation of the scattering length. This equation (7), for  $\alpha = 0$  ( $\omega_3 \rightarrow 0$ ) and  $\epsilon = 0$ , has the solitonic solution

$$u^{(s)} = \sqrt{2} A \operatorname{sech}[A(z - v\tau)] \exp \left\{ i \left( \frac{vz}{2} + A^2 \tau - \frac{v^2 \tau}{4} \right) \right\}, \quad (8)$$

where  $A$  is a constant and  $v$  is the soliton velocity. Confirmation of this model by full 3D numerical simulations is given in section 4.

Considering that in the transversal direction we have a much stronger trapped potential ( $\omega_{\perp} \gg \omega_3$ ), validating the approximation considered in equation (2), we should observe that any different modelling of the impurity in the transversal directions can only bring a multiplicative constant factor in the resulting nonlinear 1D equation. This will result in changing the absolute value of the scattering length or its local space variation (the constant  $\epsilon$ ). We should also add that the changes in the scattering length will not induce changes in the transverse mode structure, so, the integration procedure over transverse modes is still valid, and the level of applicability is the same as in the case that  $\epsilon = 0$ . If we consider modulations of the nonlinear coefficient via, for example, local variation of transverse distribution of trap potential, then the transverse modal structure will change and the 1D approximation can fail. But this is not the case we are going to consider.

The 1D Hamiltonian energy corresponding to equation (7) is given by

$$\langle H \rangle = \frac{1}{n_0} \int_{-\infty}^{\infty} dz \left[ \left| \frac{\partial u}{\partial z} \right|^2 + \alpha z^2 |u|^2 - \frac{(1 + \epsilon f(z))}{2} |u|^4 \right], \quad (9)$$

where  $n_0$  is the normalization of  $u$ , related to the number of particles  $N$  and the scattering length  $a_{s0}$ :

$$n_0 = \frac{4N|a_{s0}|}{l_{\perp}}. \quad (10)$$

The validity of the 1D approximation of the original 3D equation is expected for  $n_0^2 \ll 8$ , as shown in [7]. We should also add that in a 3D calculation given in [7, 8], it was already demonstrated that, before such limit is achieved, the system will collapse at  $n_0 = 4k_{\perp}$ , where  $k_{\perp} = 0.676$ .

We should observe that in the realistic case one has a quasi-1D (cigar-like) trap. In [11], the authors have considered the formation and propagation of matter-wave solitons, using a gas of  ${}^7\text{Li}$  atoms, in a quasi-1D trap. The frequencies used in their trap are  $\omega_{\perp} = 2\pi \times 625$  Hz and  $\omega_L = \omega_3 = 2\pi \times 3.2$  Hz, with the scattering length tuned to  $a_{s0} = -3a_0$  ( $a_0$  is the Bohr radius). The ratio of such frequencies gives  $\alpha = (\omega_3/\omega_{\perp})^2 = 2.6 \times 10^{-5}$ . In this case, as shown in [7, 8], the maximum critical number  $n_{0,\max}$  is a constant that does not depend on  $a_{s0}$ . The realistic maximum number of atoms  $N_c$  will be related to  $a_{s0}$  and the oscillator length:  $N_c|a_{s0}|/l_{\perp} \approx 0.676$ .

To study the dynamics of the soliton, perturbed by inhomogeneities, we use the following trial function [26]:

$$u = A \operatorname{sech} \left( \frac{z - \zeta}{a} \right) e^{i[\phi + w(z - \zeta) + b(z - \zeta)^2]}, \quad (11)$$

where  $A, a, \zeta, \phi, w$  and  $b$  are time-dependent variational parameters. In this case  $u$  is normalized to  $n_0 = 2aA^2$ . To derive the equations for the time-dependent parameters of the soliton, we first obtain the averaged Lagrangian

$$\bar{\mathcal{L}}(\tau) = \int \mathcal{L}(z, \tau) dz, \tag{12}$$

with

$$\mathcal{L}(z, \tau) = \frac{i}{2} \left( \frac{\partial u}{\partial \tau} u^* - \frac{\partial u^*}{\partial \tau} u \right) - \left| \frac{\partial u}{\partial z} \right|^2 - \alpha z^2 |u|^2 + \frac{1}{2} [1 + \epsilon f(z)] |u|^4. \tag{13}$$

The equations for the soliton parameters are derived from the Lagrangian  $\bar{\mathcal{L}}$ , by using the corresponding Euler–Lagrange equations. So,  $\bar{\mathcal{L}}$  is given by

$$\begin{aligned} \bar{\mathcal{L}} = & -n_0 \left[ \frac{\partial \phi}{\partial \tau} - w \frac{\partial \zeta}{\partial \tau} + \frac{\pi^2}{12} a^2 \frac{\partial b}{\partial \tau} \right] - \frac{n_0}{3a^2} - n_0 w^2 - \frac{\pi^2 n_0 a^2 b^2}{3} \\ & + \frac{n_0^2}{6a} + \epsilon \frac{n_0^2}{8a^2} F(a, \zeta) - \alpha n_0 \left( \zeta^2 + \frac{\pi^2}{12} a^2 \right), \end{aligned} \tag{14}$$

where

$$F(a, \zeta) \equiv \int_{-\infty}^{\infty} dz \frac{f(z)}{\cosh^4 \left( \frac{z-\zeta}{a} \right)}. \tag{15}$$

We also obtain the coupled equations for  $a$  and  $\zeta$ :

$$\begin{aligned} \frac{d^2 a}{d\tau^2} = & \frac{16}{\pi^2 a^3} - \frac{4n_0}{\pi^2 a^2} - \epsilon \frac{3n_0}{\pi^2 a^2} \left[ 2 \frac{F}{a} - \frac{\partial F}{\partial a} \right] - 4\alpha a, \\ \frac{d^2 \zeta}{d\tau^2} = & -4\alpha \zeta + \epsilon \frac{n_0}{4a^2} \frac{\partial F}{\partial \zeta}. \end{aligned} \tag{16}$$

The equation for the phase is not coupled with the above; it is related with the conservation of the number of atoms. When  $a$  is constant we have the well-known description of the soliton centre as the unit mass particle in an anharmonic potential, that in the present case will be given by  $U(\zeta) = -\epsilon(n_0/(4a^2))F(a, \zeta)$  (see [27]). For  $\epsilon < 0$ , to overcome such effective barrier, the velocity at  $\zeta = 0$  should be larger than  $v_c$ , where  $v_c^2 = |\epsilon|n_0/(2a^2)F(a, \zeta = 0)$ .

In order to have a more general formulation of the model, in the present section we have considered a non-zero external potential, parametrized by  $\alpha$ . One could also explore the behaviour of the soliton, by considering a more general time-dependent form of the external potential, as studied in [28]. However, in the present work our main motivation is the propagation of matter-wave bright solitons, in a 1D cigar-like trap [11], where  $\alpha = (\omega_3/\omega_{\perp})^2 = 2.6 \times 10^{-5}$  such that we will assume  $\alpha = 0$  in the following sections.

### 3. Analysis of dynamics of bright solitons under different types of inhomogeneities

#### 3.1. Point-like nonlinear inhomogeneity

Let us analyse the system of equations (16), with  $\alpha = 0$ , by first considering a delta-type inhomogeneity ( $f(z) = \delta(z)$ ), and look for the fixed points of such a system. In this case, the approximation for the inhomogeneity can be used when the characteristic scale of the inhomogeneity  $l_{\epsilon}$  is much less than the soliton scale  $l_s$ , i.e. when

$$l_{\epsilon} \ll l_s \equiv \frac{l_{\perp}^2}{N|a_{s0}|} = \sqrt{\frac{l_{\perp}^2 l_s}{N|a_{s0}|}} = \frac{1}{\sqrt{|a_{s0}| \rho_c}}, \tag{17}$$

where  $\rho_c \equiv N/(l_s l_{\perp}^2)$  is the condensate density.

From equation (15), with  $f(z) = \delta(z)$ , we obtain  $F$  and its derivatives:

$$\begin{cases} F(a, \zeta) = \operatorname{sech}^4\left(\frac{\zeta}{a}\right), \\ \frac{\partial F}{\partial a} = \frac{4\zeta}{a^2} \tanh\left(\frac{\zeta}{a}\right) \operatorname{sech}^4\left(\frac{\zeta}{a}\right), \\ \frac{\partial F}{\partial \zeta} = -\frac{4}{a} \tanh\left(\frac{\zeta}{a}\right) \operatorname{sech}^4\left(\frac{\zeta}{a}\right). \end{cases} \quad (18)$$

The fixed point for the soliton centre is given by  $\zeta = 0$ . This corresponds to the case of an atomic matter soliton trapped by the local variation of the two-body scattering length. In case the local variation corresponds to a positive scattering length ( $\epsilon < 0$ ), we should observe the soliton being reflected by the inhomogeneity. Then, the stationary width  $a_c$  can be defined by

$$a_c = \frac{8 - 3\epsilon n_0}{2n_0}. \quad (19)$$

Expanding the solution near  $a_c$ , we obtain the frequencies of small oscillations for the width  $a$  and for the centre-of-mass  $\zeta$  of the soliton, localized by the impurity. The square of such frequencies is, respectively, given by

$$\omega_a^2 = \frac{4n_0}{\pi^2} \left(\frac{2n_0}{8 - 3n_0\epsilon}\right)^3, \quad \omega_\zeta^2 = \epsilon n_0 \left(\frac{2n_0}{8 - 3n_0\epsilon}\right)^4. \quad (20)$$

In the variational approach for the soliton interacting with the impurity, we have the interaction of the oscillating internal degree of freedom (the width) with the soliton centre. As can be seen from equations (20), the frequencies of the oscillations can match for a certain value of  $\epsilon$ , with energy transfer between the two modes. So, as a result of the reflection from attractive inhomogeneity in BEC, a depinning of the soliton can occur. Note that the soliton width goes to zero and the frequencies are singular when

$$\epsilon = \epsilon_c = \frac{8}{3n_0}. \quad (21)$$

The singularity occurs when the contributions coming from the inhomogeneity and nonlinearity are equal to the contribution from the quantum pressure, as seen from equation (16). When  $\epsilon \geq \epsilon_c$  the collapse of solitary wave occurs. Here, it is interesting to observe that we have two critical numbers that are related: one of the critical number,  $k_\perp = n_{0,\max}/4 \approx 0.676$ , comes from the quasi-1D limit of a 3D calculation [8]; another is the maximum amplitude of the delta-like impurity that we have just introduced, given by equation (21). So, we can observe *the collapse* of a 1D soliton on *the attractive nonlinear* impurity. This possibility can be obtained following a dimensional analysis in the 1D Hamiltonian given in equation (9). The behaviour of the field at small widths is  $u \sim 1/L^{1/2}$ . Taking into account that  $\delta(z) \sim 1/L \sim |u|^2$ , we can conclude that the contribution of the potential energy due to the impurity is  $\sim |u|^6$ . For positive  $\epsilon$ , this term on the impurity exceeds the quantum pressure and leads to the collapse of the soliton. In real situations, the collapse will be arrested on the final stage of the evolution, when the soliton width becomes of the order of the inhomogeneity scale. Then, the delta-function approximation for the impurity will break up.

The collapse condition can also be obtained by analysing the behaviour of the second time derivative of the mean-square radius, as in [5, 29, 30]. To obtain the second time derivative of the mean-square radius, we use the Virial approach, with  $H = -\frac{\partial^2}{\partial z^2} + V$  and

$V \equiv -(1 + \epsilon\delta(z))|u|^2$ :

$$\begin{aligned}\frac{d^2}{d\tau^2}\langle z^2 \rangle &= 4 \left\langle \left[ H, z \frac{\partial}{\partial z} \right] \right\rangle = 8 \left\langle -\frac{\partial^2}{\partial z^2} \right\rangle - 4 \left\langle z \frac{\partial V}{\partial z} \right\rangle, \\ \left\langle z \frac{\partial V}{\partial z} \right\rangle &= -\frac{1}{2}\langle V \rangle + \frac{\epsilon}{2n_0}|u_0|^4, \\ \frac{d^2}{d\tau^2}\langle z^2 \rangle &= \frac{1}{n_0} \int dz \left( 8 \left| \frac{\partial u}{\partial z} \right|^2 - 2|u|^4 \right) - \frac{4\epsilon}{n_0}|u_0|^4.\end{aligned}\quad (22)$$

For the system to collapse we need  $\frac{d^2}{d\tau^2}\langle z^2 \rangle < 0$ ; implying that

$$\epsilon > \frac{1}{2|u(0)|^4} \int \left( 4 \left| \frac{\partial u}{\partial z} \right|^2 - |u|^4 \right) dz. \quad (23)$$

Using our solitonic ansatz, when  $a \rightarrow 0$ , we reach the critical limit,  $\epsilon_c = 8/(3n_0)$  that was obtained before.

In section 4, we will consider a detailed comparison of these predictions with full numerical simulations of the GP equation.

### 3.2. Interface between two BEC media

Now, we consider another interesting case of an interface between two media, such that at  $z = 0$  we have a sudden change in the two-body scattering length. Representation of the interface as a step-like function,  $\theta(z)$ , is possible since the soliton scale is much larger than the scale of the inhomogeneity. The size of the inhomogeneity is given by  $\epsilon$  in equation (7), where  $f(z) = \theta(z)$ . In this case, we have

$$\begin{cases} F(a, \zeta) = a \left[ \frac{2}{3} + \tanh\left(\frac{\zeta}{a}\right) - \frac{1}{3}\tanh^3\left(\frac{\zeta}{a}\right) \right], \\ \frac{\partial F}{\partial a} = \frac{F}{a} - \frac{\zeta}{a}\operatorname{sech}^4\left(\frac{\zeta}{a}\right), \\ \frac{\partial F}{\partial \zeta} = \operatorname{sech}^4\left(\frac{\zeta}{a}\right). \end{cases} \quad (24)$$

And, from (16) with  $\alpha = 0$ , we obtain the coupled equations:

$$\begin{aligned}\frac{d^2 a}{d\tau^2} &= \frac{16}{\pi^2 a^3} - (\epsilon + 2) \frac{2n_0}{\pi^2 a^2} - \epsilon \frac{3n_0}{\pi^2 a^2} \left[ \tanh\left(\frac{\zeta}{a}\right) - \frac{1}{3}\tanh^3\left(\frac{\zeta}{a}\right) + \left(\frac{\zeta}{a}\right)\operatorname{sech}^4\left(\frac{\zeta}{a}\right) \right], \\ \frac{d^2 \zeta}{d\tau^2} &= \epsilon \frac{n_0}{4a^2} \operatorname{sech}^4\left(\frac{\zeta}{a}\right).\end{aligned}\quad (25)$$

There is no fixed point. At the interface, the value of the width is reduced,

$$a_{\text{int}} = \frac{8}{n_0(\epsilon + 2)}, \quad (26)$$

and the frequency of oscillation of the pulse width is

$$\omega_a = \frac{n_0^2(\epsilon + 2)^2}{16\pi}. \quad (27)$$

For a constant value of  $a$ , from (25), we obtain

$$\left(\frac{d\zeta}{d\tau}\right)^2 = 2\epsilon \frac{n_0}{4a^2} F(a, \zeta) \leq \epsilon \frac{2n_0}{3a}. \quad (28)$$

When  $a = 4/n_0$ , the system (25) reduces to the single equation for  $\zeta$  describing the motion of the effective particle. Note that equation (28) describes the propagation of the centre of the optical plane of the beam, crossing the interface between two nonlinear optical media with Kerr (cubic) nonlinearities [31, 32]. If the velocity exceeds the critical value, the soliton passes through the inhomogeneity. An interesting effect, predicted in [32], can occur when the soliton crosses the interface, namely, the possibility of soliton splitting. The soliton is the solution in the first medium. In the second medium it can be considered as the initial wavepacket deviating from the solitonic solution, for this media. Applying the approach developed in [33], such initial condition will decay on few solitons plus radiation [32]. The number of generated solitons is equal to

$$n_{\text{sol}} = \mathcal{I} \left[ \frac{1}{\sqrt{2\pi}} \int_{-\infty}^{\infty} |u_0| dz + \frac{1}{2} \right], \quad (29)$$

where  $u_0$  is the initial solution for the second medium, and  $\mathcal{I}[\dots]$  stands for *integer part of*  $[\dots]$ . Thus, if we have a jump in the scattering length given by  $\Delta a_s = a_{s2} - a_{s1}$ , then the number of generated solitons in the second part of the BEC is equal to  $n_{\text{sol}} = \mathcal{I}[\sqrt{a_{s2}/a_{s1}} + 1/2]$ , where  $(1 + \epsilon) = a_{s2}/a_{s1}$  is the ratio of the atomic scattering lengths. For example, for the ratio  $9/4 < a_{s2}/a_{s1} < 25/4$  (or  $1.25 < \epsilon < 5.25$ ) we obtain two solitons in the right-hand side medium. To obtain  $n_{\text{sol}}$ , we need  $\epsilon$  such that  $n_{\text{sol}}(n_{\text{sol}} - 1) < (\epsilon + 3/4) < n_{\text{sol}}(n_{\text{sol}} + 1)$ .

### 3.3. Slowly varying inhomogeneity

In this subsection, we consider the system of equations (16) for a slowly varying (on the soliton scale) inhomogeneity, given by  $f(z) = \exp(-z^2/l_\epsilon^2)$ , with  $l_\epsilon \gg a$ . In this case, we obtain the following approximate expressions for  $F(a, \zeta)$  and its derivatives:

$$\begin{cases} F(a, \zeta) \approx \frac{4a}{3} \exp\left(-\frac{\zeta^2}{l_\epsilon^2}\right), \\ \frac{\partial F}{\partial a} \approx \frac{4}{3} \exp\left(-\frac{\zeta^2}{l_\epsilon^2}\right), \\ \frac{\partial F}{\partial \zeta} \approx -\left(\frac{8a\zeta}{3l_\epsilon^2}\right) \exp\left(-\frac{\zeta^2}{l_\epsilon^2}\right). \end{cases} \quad (30)$$

There is a fixed point at  $\zeta = 0$ , given by

$$a_c = \frac{4}{n_0(1 + \epsilon)}. \quad (31)$$

The soliton is trapped by the inhomogeneity for positive  $\epsilon$ . In the trapped regime, due to internal degrees of freedom, oscillations of the width and oscillations of the centre of mass occur. The corresponding frequencies are, respectively, given by

$$\omega_a = \frac{n_0^2(1 + \epsilon)^2}{4\pi}, \quad (32)$$

and

$$\omega_\zeta = \sqrt{\frac{\epsilon(1 + \epsilon)}{6}} \frac{n_0}{l_\epsilon} \xrightarrow{l_\epsilon \gg a} 0. \quad (33)$$

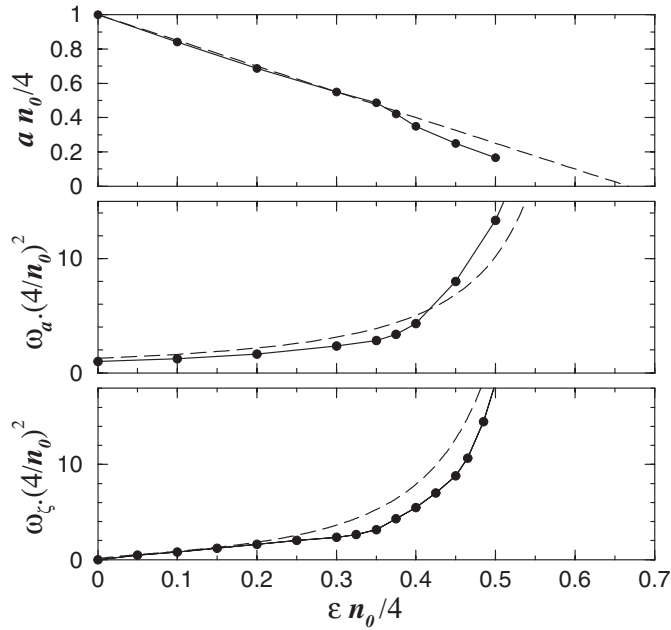


**Figure 1.** The width  $a$ , the frequency of the width oscillations  $\omega_a$  and the frequency of the soliton centre-of-mass oscillations  $\omega_z$  are shown in terms of the strength of the nonlinear impurity  $\epsilon$ . All the quantities are dimensionless and given with appropriate scaling in terms of the normalization  $n_0$ . Solid line with bullets corresponds to full numerical solution, and dashed line to the corresponding variational approach.

Considering an experiment, as in [10, 11], with the scattering length of the order of  $-3a_0$ , and with a variation of about one  $a_0$ , we obtain  $\epsilon \sim 1/3$ . Taking the critical number  $k_{\perp} = n_0/4 = 0.676$ , we obtain  $\omega_a \approx 1$ , which implies that the characteristic frequency of oscillations of the soliton width is close to  $\omega_{\perp}$  (as the frequencies are given in this unit). And the frequency of oscillation of the centre of mass goes to zero with  $l_{\epsilon} \gg a$ , as  $\omega_z \sim (0.6/l_{\epsilon})$ . We note that the length unit  $l_{\perp}$ , for  ${}^7\text{Li}$  with  $\omega_{\perp} = 2\pi \times 625$  Hz, is about  $1.5 \mu\text{m}$ . The above values for the oscillation frequencies can be verified in an elongated BEC experiment, with different values of atomic scattering length, as in the configuration discussed in [23].

#### 4. Numerical simulations and general discussion

##### 4.1. Numerical 1D results and variational approach

Our approach for pulses deviating from the exact soliton solution is interesting from the experimental point of view, considering the difficulty in producing exact solitonic solutions. Of particular interest is the non-trivial case of nonlinear Dirac-delta impurity ( $f(z) = \delta(z)$ ), where we made detailed comparison between the variational and full numerical solution of the GP equation. For the full numerical solution this 1D Dirac-delta function is obtained as in [19], i.e. approximated by a rectangular shape, with base  $\Delta z$  and height  $1/\Delta z$ , where  $\Delta z$  is the grid step.

In figure 1, we are comparing the variational results with the numerical results for a wavefunction trapped by the inhomogeneity. For each  $\epsilon$ , given in the  $x$ -axis, we obtain the results for fixed points of the width ( $a$ ), for the width oscillation frequencies ( $\omega_a$ ) and for the

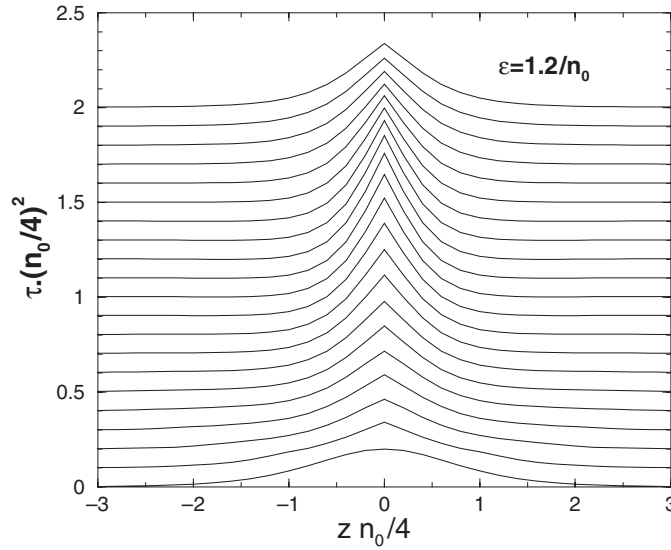


**Figure 2.** Density profile evolution for a fixed value of the amplitude of the delta-like impurity  $\epsilon$ , with arbitrary  $n_0$ , in a projected 3D plot. Each line corresponds to a fixed value of  $\tau$  given in the  $y$ -axis, with the corresponding amplitudes in arbitrary scale, relative to the one at  $\tau = 0$ .  $\tau$  and  $z$  are dimensionless quantities, as given in the text. At  $z = 0$ , we observe the oscillation of the amplitude, starting from the normal one and going to the nonlinear localized one. For larger  $\epsilon$ , not shown in this figure, one can also observe the emission of radiation.

centre-of-mass oscillation frequencies ( $\omega_\zeta$ ). The plots in the three frames are obtained for arbitrary values of  $n_0$  (where the maximum is about  $8/3$ , according to [8]), after considering a rescaling in the equations for the width (19) and frequencies (20); and also for  $\epsilon$ , such that in the  $x$ -axis we consider  $(n_0/4)\epsilon$ . From equation (21), one obtains that  $\epsilon_c(n_0/4) = 2/3$ . As shown in this figure, the variational results are supported by the full numerical calculation. We should note that the variational ansatz starts to fail near the critical point, in comparison with the exact calculation. This is clear from the results obtained for the frequencies as well as for the width. However, we should mention that the precision of some points, shown for the exact calculations of the width, is disturbed by radiations. This numerical problem does not occur in the calculation of the frequencies.

In figure 2, we show numerical simulations of the wave profile. Each line corresponds to a fixed value of  $\tau$  given in the  $y$ -axis, with the amplitudes in arbitrary scale relative to the one at  $\tau = 0$ . After strong emission of radiation, the wave profile evolves into the so-called *nonlinear localized mode*. This mode represents an *exact* solution of the GP equation with nonlinear impurity (7) and it is the nonlinear *standing* atomic matter wave. The solution,

$$u^{(ni)} = \sqrt{2}a \operatorname{sech}[a|z| + \beta] e^{ia^2\tau}, \tag{34}$$

where

$$\beta \equiv \beta(\epsilon, a) \equiv \operatorname{sign}(\epsilon) \ln(2|\epsilon|a + \sqrt{1 + 4\epsilon^2 a^2})^{1/2}, \tag{35}$$

can be obtained by using the solution of the homogeneous equation with the requirement of the field continuity at the inhomogeneity and satisfying the jump condition in the first derivative [29]. The normalization of equation (34) is

$$N^{(ni)} = \int |u^{(ni)}|^2 dz = 4a \left[ 1 - \frac{2\epsilon a}{\sqrt{1 + 4\epsilon^2 a^2} + 1} \right]. \tag{36}$$

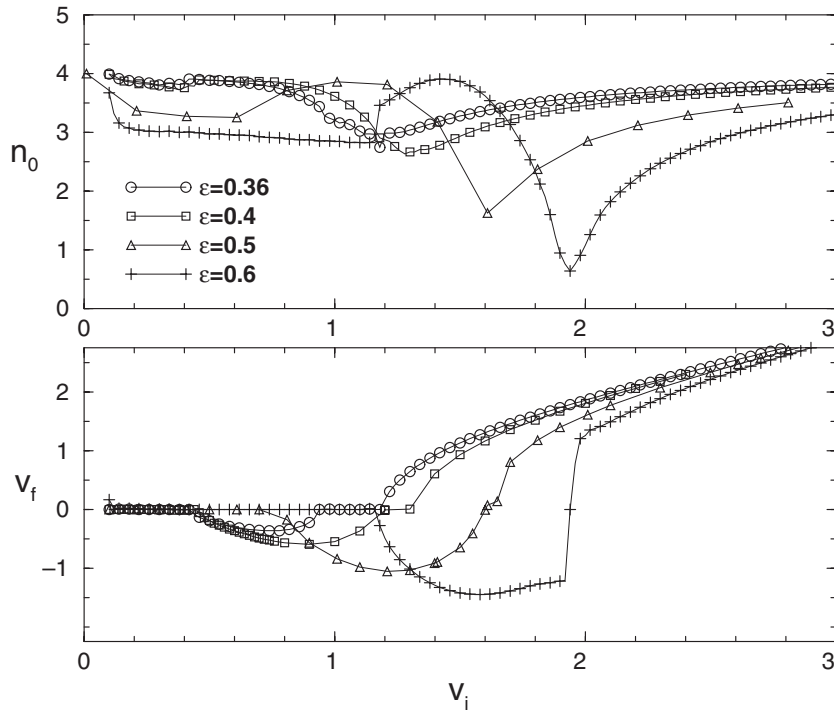


**Figure 3.** Numerical simulations of the full GP equation, showing the dependence of  $n_0$ , related to the number of atoms  $N$  (top frame), and final velocity  $v_f$  (bottom frame), with respect to the initial velocity  $v_i$ . The results of both frames are shown for different values of  $\epsilon$ , as indicated inside the top frame. The initial value (for  $v_i = 0$ )  $n_0 = 4$  can be rescaled as explained in the text. All the quantities are dimensionless.

For small amplitude (or small impurity strength  $|\epsilon|$ ),

$$N^{(ni)} \approx 4a(1 - \epsilon a). \quad (37)$$

At large amplitudes, we have  $N^{(ni)} \rightarrow 2/\epsilon$  for  $\epsilon > 0$ , and  $N^{(ni)} \rightarrow 8a$  for  $\epsilon < 0$ . Note that for  $\epsilon < 0$ , we have a solution with a two bump structure for the nonlinear localized mode. As shown in [29], this mode is unstable. Here, we have considered only the case  $\epsilon > 0$ .

We also investigate the dynamics of the matter-wave soliton interacting with inhomogeneity, studying different regimes of propagation for several values of  $\epsilon$ . In figure 3, we present the results of numerical simulations for the final velocity ( $v_f$ ) versus the initial velocity ( $v_i$ ) of the soliton, considering different strengths  $\epsilon$  for the delta-like inhomogeneity. In figure 3 and in the next numerical results, considering the general application of 1D NLSE with nonlinear impurity, we took  $N|a_{s0}|/l_{\perp} = n_0/4 = 1$ , that can easily be rescaled to a value lesser than 0.676, consistent with the BEC quasi-1D results. Considering a factor  $\xi$  for the rescaling, as a general rule, we have the following transformations:

$$\epsilon \rightarrow \epsilon\xi, \quad \{\text{length}\} \rightarrow \{\text{length}\}\xi, \quad \{\text{time}\} \rightarrow \{\text{time}\}\xi^2. \quad (38)$$

We should note that the rescaling applied in figures 1 and 2 was such that  $\xi = n_0/4$ . In this case, for the velocities, one should make the replacement  $v \rightarrow v(4/n_0)$  in the plots.

As observed in figure 3, a region for the velocities exists where the *attractive* nonlinear impurity reflects the soliton. In the model involving the constant width approximation, this

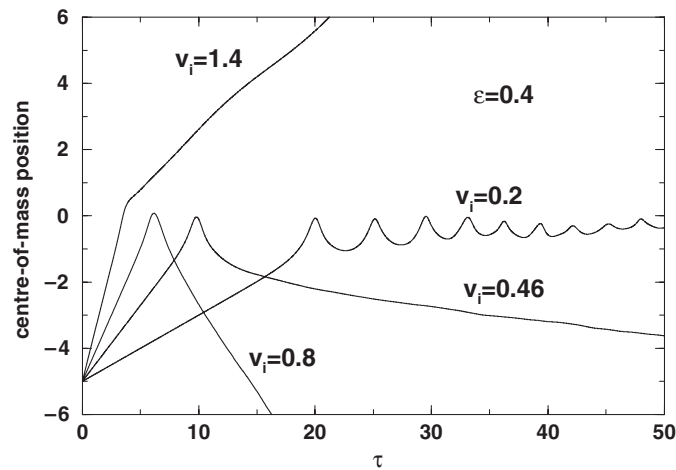


**Figure 4.** For a fixed value of  $\epsilon = 0.4$ , we present a full numerical solution of the GP equation, with the time evolution of the centre-of-mass position, considering different values of the initial velocity, as given inside the frame. The results, given for  $n_0 = 4$ , can be rescaled as explained in the text. All the quantities are dimensionless.

region corresponds to the trapped soliton. The numerical results show that, in all the cases that we have analysed (for all values of  $\epsilon$ ), one window (interval) exists in the velocity axis corresponding to the reflection of the soliton. By increasing  $\epsilon$ , this window is shifted to larger initial velocities. In [19], many windows were found in the interaction of a sine-Gordon kink with an attractive defect, corresponding to a resonance with local mode. From the variation of the number  $n_0$  (related to the number  $N$  by equation (10)) with respect to the initial velocity  $v_i$  (top frame of figure 3), one can also observe strong wave emissions by the soliton, when  $\epsilon$  increases and tends to the critical value (see also [29]). This picture resembles the collapse in 2D BEC with attractive interaction.

In order to compare with the results given in the lower frame of figure 3, we present in figure 4 full numerical calculations of the time evolution of the centre-of-mass position. We took a fixed value of  $\epsilon = 0.4$ , with different values of the initial velocity.

We can observe different regimes for the soliton interaction with the nonlinear impurity: reflection, transmission and trapping. The most interesting noted effect is the reflection of the soliton by the attractive potential at the velocity interval  $0.42 < v_i < 1.2$ .

Through the results given in figure 5, one can also observe that numerical simulations of the variational equations (16)–(18) reproduce only qualitatively the behaviour observed in the full numerical solution of the GP equation. In figure 5, we observe the behaviour of the final velocity as a function of the initial velocity, for  $\epsilon = 0.4$  and  $n_0 = 4$ . We represent the variational results obtained from (16) with solid line and the full numerical solution with dashed line. We note that the full numerical solution shows a window, between two trapped regions, where the soliton is reflected by the impurity. The variational result shows the window of reflection starting for smaller initial velocities and, instead of a trapped region, a more complicated dynamics near the points where the regime of reflection starts or finishes. For  $v_i$  between 0.5 and 1.0, the observed noise is a kind of behaviour that occurs for a system of variational equations. Similar behaviour has also been observed in the problem of kink interaction with impurity in a nonlinear system described by the sine-Gordon equation with

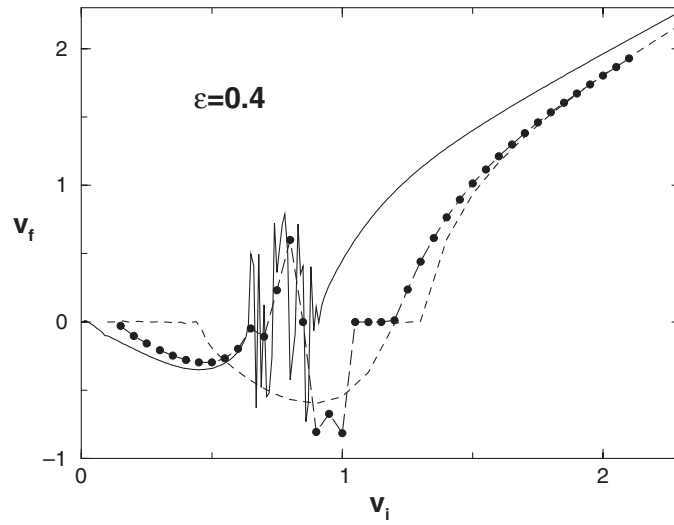


**Figure 5.** Comparison between variational and full numerical simulations of the GP equations, considering point-like nonlinear impurity [ $f(z) = \delta(z)$ ] with  $\epsilon = 0.4$ . We plot the final velocity  $v_f$  versus the initial velocity  $v_i$ . With dashed line we show the full numerical results, obtained from equation (7) with  $\alpha = 0$ . Results for the variational equations (16) are shown with a solid line, and those, including a damping factor as explained in the text with a dot-dashed line. The results, obtained for  $n_0 = 4$ , can be rescaled as explained in the text. All the quantities are in dimensionless units.

a local defect [18]. One can improve the variational approach by taking into account the influence of radiative friction on the soliton motion on the impurity as given in [35]. In the second line of (16), by adding a term  $c\zeta^2(d\zeta/d\tau)$  (where  $c$  is a phenomenological constant), the resulting effect is an oscillation damping ( $\sim 1/\sqrt{\tau}$ ) that will improve the variational results as compared with full numerical solutions. By using  $c = 0.01$ , we can also observe the second trapped region close to the exact results. See the curve with solid circles in figure 5.

Our variational approach includes chirp, presenting internal degrees of freedom. The impurity couples the internal degrees of freedom with the translational degrees of freedom, so energy exchange between modes occurs, such that we have reflection or transmission for the parameters where the effective particle method predicts a trapped regime [32].

#### 4.2. Full numerical 3D results

To check the validity of the 1D reduction, in the case of point-like nonlinear impurity, we also performed full 3D numerical calculations. The ground-state solutions were obtained by solving the original 3D equation, given in (1), and by comparing them with the corresponding exact solution of the 1D equation. In dimensionless units, in the limit  $\alpha = 0$ , considering the definitions given in (4), (6) and (10), the 3D equation solved numerically can be written as

$$i\frac{\partial\psi}{\partial\tau} = -\frac{\partial^2\psi}{\partial x^2} - \frac{\partial^2\psi}{\partial y^2} - \frac{\partial^2\psi}{\partial z^2} + (x^2 + y^2)\psi - 2\pi n_0[1 + \epsilon\delta(z)]|\psi|^2\psi, \quad (39)$$

where  $\psi \equiv \psi(\vec{x}_\perp, z, \tau) \equiv \sqrt{l_\perp^3/N}\Psi(\vec{r}, t)$  with  $\vec{x}_\perp \equiv (x, y) \equiv (x_1/l_\perp, x_2/l_\perp)$ . The ground-state numerical solutions are obtained using imaginary time propagation and cylindrical coordinates, as described in [34]. Our results are given in figure 6, for  $2\pi n_0 = 5$  and 10, showing the ground-state behaviour as a function of  $z$ , at the origin in the transversal

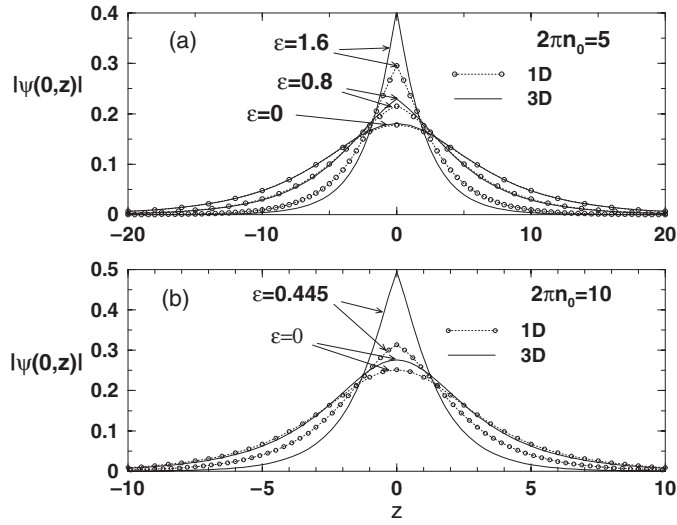


**Figure 6.** In the above figures (a) and (b) we show results for the ground-state solutions obtained by solving the original 3D equation (1) (solid line), in comparison with the corresponding 1D solutions (dashed-lines with dots), given by (34). All the quantities are in dimensionless units:  $z = x_3/l_\perp$ , with  $l_\perp \equiv \sqrt{\hbar/(m\omega_\perp)}$ , and the wavefunction is normalized to 1, such that  $|\psi(0, z)|^2 \equiv |\Psi(\vec{r}, t)|_{|\vec{r}=x_3}^2 (l_\perp^3/N)$ . The parameters we have considered,  $n_0$  and  $\epsilon$ , are given inside the figures.

directions. We observe a critical value for the parameter  $\epsilon$  of the nonlinearity, such that for larger  $\epsilon$  the system collapses. For example, in the case that  $2\pi n_0 = 10$ , the system collapses if we consider  $\epsilon \geq 0.45$ . And, in the case that  $2\pi n_0 = 5$ , the system collapses for  $\epsilon \geq 1.65$ . The deviation from the analytical prediction, that one can observe particularly in the case of  $2\pi n_0 = 10$ , is connected with the fact that the contribution of nonlinear term in the transverse direction becomes comparable with the transverse harmonic potential. So, as explained before, the 1D approximation is expected to be violated.

We found illustrative to present in figure 7 the relation between the two critical limits:  $k_\perp(\epsilon) \equiv n_{0,\max}/4$  and the inhomogeneity parameter  $\epsilon_c$ . When  $\epsilon = 0$  we have  $k_\perp = N_c |a_{s0}|/l_\perp \approx 0.676$  [7, 8]. As the parameter  $\epsilon$  of a delta-like impurity increases, the corresponding negative value of the nonlinear term of equation (1) also increases, and the maximum number of atoms  $N_c$  decreases (considering fixed  $a_{s0}$  and  $l_\perp$ ).

The agreement of 1D with 3D model was also verified in a dynamical calculation, using a specific example where the soliton reflects at the impurity. To obtain numerically stable results for equation (39), we use a similar code as described in [8], with  $40 \times 40 \times 120$  space grid points and time step  $\tau = 0.01$ , propagating in real time. The results of the 3D dynamical calculation are shown in figure 8, considering the distance of the impurity from the origin to be  $\Delta z = 25$ . In this case, we have considered parameters that correspond to the 1D parameters of figures 3 and 5 ( $n_0 = 4$ ,  $\epsilon = 0.4$ ,  $v_i = 0.8$ ). After proper rescaling (see equation (38)), with  $n_0 = 5/(2\pi)$ , we obtain  $\epsilon = 2$  and  $v_i = 0.16$ . We have presented several plots of the soliton profile using time steps such that  $\Delta\tau = 50$ . We observe the soliton reflecting at the impurity, following the same behaviour as in the 1D numerical results. From an analysis of the critical limits given in figure 7, one should expect that for  $\epsilon > 1.6$  the system will collapse. However, the results of figure 7 are obtained for the ground state in static calculations. The critical limits can be increased to some extent when one considers a dynamical calculation with some initial velocity. This is shown in figure 8, using full 3D numerical evolution with  $\epsilon = 2$ .

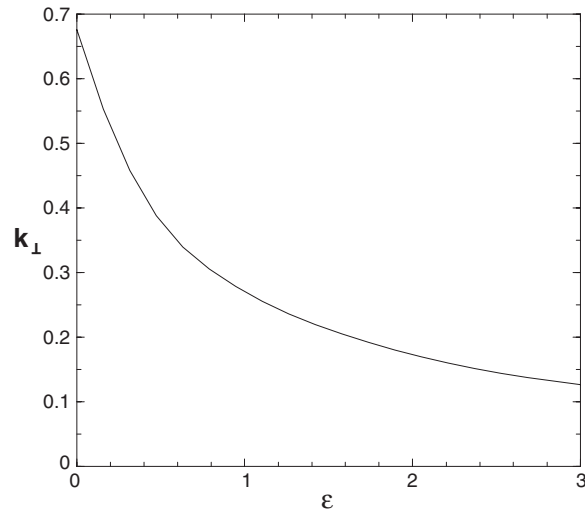


**Figure 7.** Plot of the relation between the critical numbers  $k_{\perp}$  and  $\epsilon_c$ . The maximum number of atoms  $N_c$  is given by  $k_{\perp} = N_c |a_{s0}| / l_{\perp}$ , and  $\epsilon$  is the impurity parameter for delta-like inhomogeneity. The curve shows the limit between two regions for the condensate: the lower part is the allowed region and the upper part is the collapsing region. The results are obtained using full 3D numerical calculation.

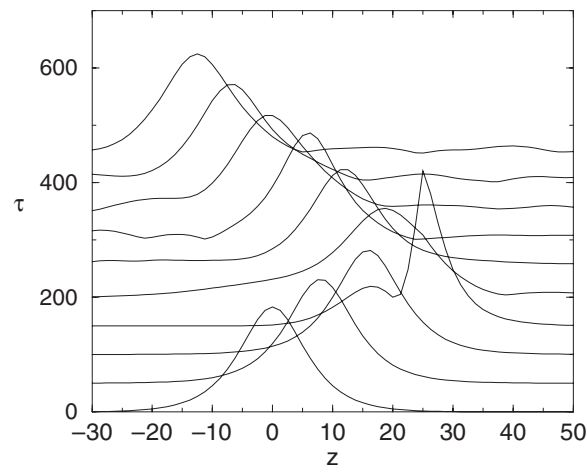


**Figure 8.** Three-dimensional numerical evolution of a soliton reflecting at an impurity placed at the position  $z = 25$ , considering  $2\pi n_0 = 5$ , initial velocity  $v_i = 0.16$  and  $\epsilon = 2$ , for the case of delta-like impurity. Each line represents the magnitude of the wavefunction  $\psi(x_{\perp} = 0, z, \tau)$  in arbitrary scale, for a fixed value of the dimensionless time  $\tau$ , given in the y-axis. All the quantities are in dimensionless units.

## 5. Conclusion

In this work, we have investigated the dynamics of bright matter-wave solitons in BEC systems with cigar-type geometry and attractive interactions. The inhomogeneities can appear in a BEC due to the existence of regions in space with different values of the two-body atomic scattering

length  $a_s$ . Indeed, by an appropriate value of the external magnetic field, one can alter the atomic scattering length [23, 24]. So, if we apply locally an external magnetic field close to the resonance value, we can obtain a local variation in the scattering length. Three kinds of inhomogeneities in the spatial distribution of  $a_s$  have been studied: local point-like, jump type and smooth (broad) type. The first type has been modelled by a Dirac-delta function, that will result in a modulation of the nonlinear term in the GP equation, corresponding to the so-called nonlinear impurity in the nonlinear Schrödinger equation. The second type corresponds to a sudden variation of the two-body scattering length that affects the amplitude of the nonlinear term in the GP equation. It corresponds to the case that the BEC system is divided into two parts with different values of  $a_s$  (see discussion of recent experiment in [23]). We have also discussed a third type of inhomogeneity that was modelled by a smooth Gaussian function. Detailed numerical simulations are given in section 4, considering the specific and non-trivial case of nonlinear Dirac-delta impurity.

The present investigation of the local variation in space of the atomic scattering length shows that different regimes of the soliton interaction with the nonlinear impurity are possible: trapping, reflection and transmission regimes. The most interesting effect is the reflection of the atomic soliton by the attractive nonlinear impurity. We have also verified the occurrence of collapse of the soliton on the attractive impurity, when the strength of the impurity (or the initial number of atoms) exceeds a certain critical value, *even in true 1D*. This effect in 1D BEC resembles the collapsing phenomena that occur in 2D BEC. By using the time-dependent variational approach we obtain a good description of the collapsing phenomena and, qualitatively, the reflection and trapping dynamics. The usual 3D collapse of the ground state has the critical number of atoms reduced by increasing the strength of the impurity.

The present approach can be more easily implemented in optically induced Feshbach experiments, as discussed in [23], with optimistic perspectives of applications in current experiments with ultracold atoms. The physical parameters can be estimated by using the optical method for the variation of the scattering length [23]. By focusing a laser beam, or using a mask, we can define a region  $l_\epsilon$  where the scattering length  $a_s$  varies, as discussed in section 3.2 for the case of a smooth varying inhomogeneity. For the case of a sudden variation of the two-body scattering length, represented by a nonlinear jump inhomogeneity, by analogy with a nonlinear optical problem [32], we presented the condition for the multiple bright matter soliton generation.

In section 4, we presented our main results considering the particular interesting case of nonlinear impurity. In the subsection 4.1. we analyse 1D full numerical results in comparison with the variational approach. In the subsection 4.2., we show that full numerical 3D calculation supports the previous 1D results.

Finally, we would like to emphasize that the problem we have studied in the present work has important applications for the control of parameters of bright atomic matter solitons and for the generation of solitons in quasi-1D BEC. Another area of possible applications is the nonlinear photonic crystals [29].

## Acknowledgments

The authors are grateful to Professor A M Kamchatnov for useful discussions and comments. This work was partially supported by Fundação de Amparo à Pesquisa do Estado de São Paulo (FAPESP). Part of this work was done by using the resources of the LCCA—Laboratory of Advanced Scientific Computation of the University of São Paulo. AG and LT are grateful for partial support from Conselho Nacional de Desenvolvimento Científico e Tecnológico.

## References

- [1] Dalfovo F, Giorgini S, Pitaevskii L P and Stringari S 1999 *Rev. Mod. Phys.* **71** 463
- [2] Meystre P 2002 *Atom Optics* (Berlin: Springer)
- [3] Denschlag J *et al* 2000 *Science* **287** 97  
Burger S *et al* 1999 *Phys. Rev. Lett.* **83** 5198
- [4] Ruprecht P A, Holland M J, Burnett K and Edwards M 1995 *Phys. Rev. A* **51** 4704
- [5] Gammal A, Frederico T, Tomio L and Abdullaev F Kh 2000 *Phys. Lett. A* **267** 305
- [6] Reinhardt W P and Clark C W 1997 *J. Phys. B: At. Mol. Opt. Phys.* **30** L785
- [7] Pérez-García V M, Michinel H and Herrero H 1998 *Phys. Rev. A* **57** 3837
- [8] Gammal A, Tomio L and Frederico T 2002 *Phys. Rev. A* **66** 043619
- [9] Frantzeskakis D J, Theocharis G, Diakonov F K, Schmelcher P and Kivshar Y S 2002 *Phys. Rev. A* **66** 053608
- [10] Khaykovich L *et al* 2002 *Science* **296** 1290
- [11] Strecker K E, Partridge G B, Truscott A G and Hulet R G 2002 *Nature* **417** 150
- [12] Carr L D and Castin Y 2002 *Phys. Rev. A* **66** 063602
- [13] Khawaja U A I, Stoof H T C, Hulet R G, Strecker K E and Partridge G B 2002 *Phys. Rev. Lett.* **89** 200404
- [14] Abdullaev F Kh, Baizakov B B, Darmanyan S A, Konotop V V and Salerno M 2001 *Phys. Rev. A* **64** 043606
- [15] Trombettoni A and Smerzi A 2001 *Phys. Rev. Lett.* **86** 2353
- [16] Forinash K, Peyrard M and Malomed B 1994 *Phys. Rev. E* **49** 3400
- [17] Cao X D and Malomed B A 1995 *Phys. Lett. A* **206** 177
- [18] Goodman R H, Holmes P J and Weinstein M I 2002 *Physica D* **161** 21 (*Preprint nlin.PS/0203057 v1*)
- [19] Kivshar Y S, Fei Z and Vazquez L 1991 *Phys. Rev. Lett.* **67** 1177
- [20] Abdullaev F Kh, Kamchatnov A, Konotop V V and Brazhnyi V 2003 *Phys. Rev. Lett.* **90** 230402
- [21] Abdullaev F Kh and Salerno M 2003 *J. Phys. B: At. Mol. Opt. Phys.* **36** 2851
- [22] Kevrekidis P G, Theocharis G, Frantzeskakis D J and Malomed B A 2003 *Phys. Rev. Lett.* **90** 230401
- [23] Fatemi F K, Jones K M and Lett P D 2000 *Phys. Rev. Lett.* **85** 4462
- [24] Timmermans E, Tommasini P, Hussein M and Kerman A 1999 *Phys. Rep.* **315** 199
- [25] Stoof H T C 1997 *J. Stat. Phys.* **87** 1353
- [26] Anderson D 1983 *Phys. Rev. A* **27** 3135
- [27] Abdullaev F Kh 1994 *Theory of Solitons in Inhomogeneous Media* (New York: Wiley)
- [28] Nogami Y and Toyama F M 1994 *Phys. Rev. E* **49** 4497
- [29] Sukhorukov A A, Kivshar Yu S, Bang O, Rasmussen J J and Christiansen P L 2001 *Phys. Rev. E* **63** 036601
- [30] Tsurumi T and Wadati M 1999 *J. Phys. Soc. Japan* **68** 1531
- [31] Nesterov L A 1988 *Opt. Spectrosc.* **64** 694
- [32] Aceves A B, Moloney J V and Newell A C 1989 *Phys. Rev. A* **39** 1809  
Aceves A B, Moloney J V and Newell A C 1989 *Phys. Rev. A* **39** 1828
- [33] Zakharov V E, Manakov A V, Novikov S P and Pitaevskii L P 1980 *Theory of Solitons* (Moscow: Nauka)  
Novikov S P, Manakov A V, Pitaevskii L P and Zakharov V E (ed) 1984 *Theory of Solitons* (New York: Consultant Bureau) (Engl. Transl.)
- [34] Gammal A, Frederico T and Tomio L 2001 *Phys. Rev. A* **64** 055602
- [35] Lakoba T I and Kaup D J 1997 *Phys. Rev. E* **56** 6147